

PFC/JA-90-43

**Induction Linac Driven Relativistic
Klystron and Cyclotron Autoresonance
Maser Experiments**

Goodman, D.L.; Birx, D.L.

Science Research Laboratory, Somerville, MA 02143

Danly, B.G.

Plasma Fusion Center
Massachusetts Institute of Technology
Cambridge, MA 02139

December 1990

This work was supported by DARPA and monitored by NSWC under contract N60921-88-C0234 and by the U.S. Department of Energy, Office of Basic Energy Sciences, under contract DE-FG02-89ER14052.

Induction linac driven relativistic klystron and cyclotron autoresonance maser experiments

D.L. Goodman, D.L. Birx

Science Research Laboratory, Somerville, MA 02143

B.G. Danly

MIT Plasma Fusion Center, Cambridge, MA 02139

ABSTRACT

Design and experimental results are presented from two high power microwave generation experiments utilizing a high repetition rate induction linac generated electron beam. A relativistic klystron has generated more than 100 MW microwave pulses in X-band for 50 ns without pulse shortening or breakdown. Design studies for the first cyclotron autoresonance maser (CARM) amplifier using an induction linac electron beam are also presented.

INTRODUCTION

There is considerable interest in high power, high repetition rate microwave sources in the 10–20 GHz range with power requirements exceeding 100 MW. Applications for such devices include RF sources for driving high gradient structures in the next generation of accelerators^{1–3} and for directed energy applications.⁴

Progress in two high power microwave experiments using a high repetition rate induction linac generated electron beam is reported in this paper. An induction linac driven relativistic klystron in operation at the MIT Plasma Fusion Center has produced 11.4 GHz 50 ns microwave pulses at power levels exceeding 100 MW in a burst mode repetition rate of 1 kHz. A cyclotron autoresonance maser (CARM) amplifier also utilizing the 500 Amp, 500 keV electron beam is now in fabrication and expected to produce 25 MW at 17 GHz. Details of induction linac operation, klystron microwave measurements and the CARM amplifier design are included in this paper.

Both experiments utilize a 500 kV, 500 A electron beam produced by the Science Research Laboratory SNOMAD-II induction accelerator. The accelerator injector includes an all solid state pulsed power unit, four induction accelerator cells, thermionic dispenser cathode and water cooled anode. The relativistic klystron is designed to produce 100 MW, 50 ns pulses using a high group velocity, water cooled, tapered phase velocity traveling wave structure as the output stage, avoiding high electric field strengths in the output cavity. RF power measurements are made using a calibrated directional coupler. A 6 kG room temperature magnet with adjustable axial field profile provides beam focussing and transport. Experimental data presented in this paper includes electron linac beam characterization studies, beam transport measurements, RF power measurements as a function of linac parameters, microwave spectral measurements and reports on high repetition rate (> 1000 pps) operation.

In addition to the relativistic klystron, a 17 GHz Cyclotron Autoresonance Maser (CARM) amplifier experiment is planned. The CARM amplifier will utilize the induction linac electron beam, with parameters of 500 keV and 500 A. CARM amplifiers are of interest as possible drivers for future high-frequency RF linear accelerators. The planned experiment has theoretical output powers as high as $P_{RF} \sim 80$ MW and $\eta \leq 32\%$ efficiency. The design of the CARM, including beam transport calculations and expected gain and operating parameters are also presented in this paper.

ELECTRON BEAM GENERATION AND MEASUREMENTS

The pulsed power for both klystron and CARM experiments is produced by the Science Research Laboratory SNOMAD-II 150 J/pulse, 125 kV, 5 kHz solid state induction linac driver, providing power to four induction accelerator cells, and producing a 500 kV, 500 Amp beam for 50 ns. The pulsed power unit requires 500 Vdc prime power, and is capable of powering up to 16 accelerator cells for a beam energy of 2 MeV. Configured as an injector, with a stainless steel cathode stalk threading the four induction accelerator cells, the accelerator consists of pulsed power unit, accelerator cells, thermionic cathode and water cooled anode. The thyratrons or spark gaps used for switching in previous generations of accelerators have been replaced by an all solid state design using SCR's. A circuit diagram for the SNOMAD-II accelerator is shown in Figure 1.

The input voltage is split into multiple arms, each completely isolated from the other, allowing the SCR's to perform individually. Four stages of nonlinear saturable inductors labelled L1-L4, step up transformers T1 and T2 and intermediate storage capacitors C1-C3 are shown. The four stage magnetic pulse compression system shown in Figure 1 produces the 125 kV, 50 ns pulses to drive the four accelerator cells. The all solid state design allows operation at high repetition rate (> 1 kHz) for long machine lifetime ($> 10^{11}$ shots). Figure 2 shows the command resonant charging waveform measured by a capacitive voltage probe located near capacitor C1. The figure shows that a repetition rate of 1000 pps has been achieved. By cooling and circulating the high voltage insulation oil, the accelerator can operate continuously at this high repetition rate.

The electron beam produced by the 3.5 inch diameter thermionic cathode is compressed to a beam radius of $r_b \sim 4$ mm and transported through the klystron tube using a 6 kG room temperature solenoidal magnet. The magnetic field at the cathode is limited to 40 G using a bucking coil and iron pole piece producing the large compression ratio. Figure 3 shows an EGUN electron ray trajectory⁵ simulation for the gun geometry used in both the klystron and CARM experiments. The magnetic field geometry shown was obtained by experimentally optimizing the microwave output power. The axial and radial scales are 2 mm per mesh unit.

Electron beam voltage and current waveforms are shown in Figure 4. The voltage is measured with a capacitive probe and the current measured using a Faraday cup. As seen in Figure 4, a current of 500 Amps at a beam voltage of 600 kV with a full width at half maximum (FWHM) of 45 ns has been measured.

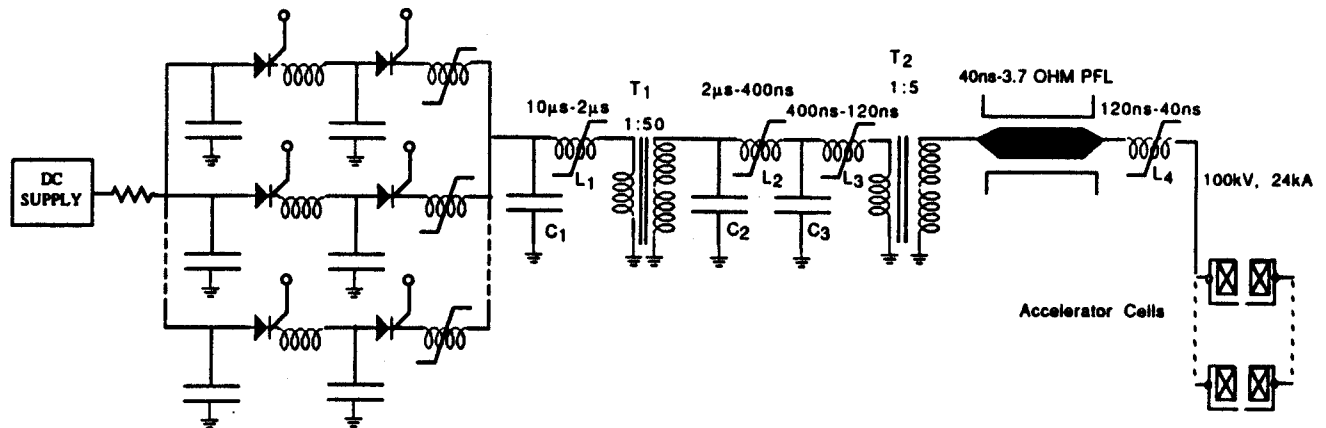


FIG. 1. The circuit diagram for the SNOMAD-II linear induction accelerator driver is shown. The saturable inductors L1-L4 allow pulse compression from the $10 \mu\text{s}$ to the 50 ns timescale.

RELATIVISTIC KLYSTRON EXPERIMENTS

Figure 5 shows microwave power measurement using a calibrated directional coupler and RF diode. As seen in Figure 5, the full design power of 100 MW at 11.4 GHz has been produced with a FWHM of nearly 50 ns. This full power operation was achieved without pulse shortening or RF breakdown seen in the input and output cavities of other klystron experiments.⁶ Use of a traveling wave output section reduced the maximum output cavity electric field to 230 kV/cm at 100 MW RF power, and is partially responsible for breakdown-free operation. Details of the TW output design have been described elsewhere.⁷ Relativistic klystron design parameters are listed in Table I.

Figure 6 shows the scaling of klystron microwave output power with voltage. The solenoidal transport magnets were adjusted to maximize RF output at each operating voltage. The best fit microwave power scaling is $P_{RF} \propto V^{3.6}$. The microwave output power can be expressed as $P = (I_{RF}^2)Z/2$, where Z is the TW structure impedance and I_{RF} is the modulated current. For space charge limited diode emission, $I \sim V^{3/2}$, and since we expect I_{RF} to scale with I , we find $P \propto V^3$. The tapered phase velocity TW output section was designed to operate at energies ≥ 460 kV, and is less efficient at lower voltages. Thus the experimental scaling of $P_{RF} \propto V^{3.6}$ shown in Figure 6 is reasonable.

The frequency spectrum of the microwave power from the relativistic klystron was measured using a calibrated commercial spectrum analyzer and a sensitive surface acoustic wave (SAW) dispersive delay line. The SAW device has a dispersive delay time of 50 MHz per 1 μ s, allowing frequency peak detection at the theoretical bandwidth limit for these 50 ns pulses. Because the traveling wave output section has a variety of resonances, single moded operation is not guaranteed, but is important for many applications especially advanced accelerators where the phase slippage is limited to a fraction of a degree.

Figures 7 and 8 show frequency spectra collected using the spectrum analyzer. When the drive frequency is 11.430 GHz (Figure 7) a single peak centered slightly below the drive frequency appears. If the drive frequency is lowered below the nominal operating frequency to 11.400 GHz (Figure 8), a second group of peaks centered at 11.710 GHz appears. Note that the main peak moved with the drive frequency,

Beam Energy	500 kV
Beam Current	500 Amps
Pulse Length	50 ns
Repetition Rate	1000 pps
Klystron Frequency	11.4 GHz
Peak RF Power	100 MW
Power Gain	50 dB
Beam Diameter	8-9 mm
Solenoidal Field	6 kG
Overall Length	48 in
TW Output Cavity	
Electric Field	230 kV/cm
Operating Pressure	$< 5 \times 10^{-7}$ Torr

Table I: Summary of the relativistic klystron operating parameters.

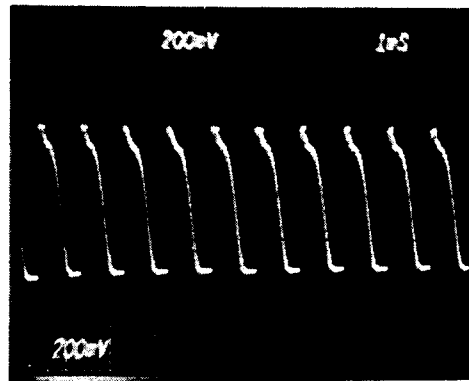


FIG. 2. Repetition rates exceeding 1 kHz have been achieved for periods of seconds in the SNOMAD-II induction linear accelerator. The command resonant charging waveform at a timescale of 1 ms/div is shown.

indicating that the microwave tube is operating as an amplifier. The second group of peaks are near the traveling wave output section π mode. Their presence when the drive is mistuned indicates both the wide gain-bandwidth of the system as well as the multimode nature of the TW output. The microwave wave form shape also depends on the drive frequency, with the widest pulse width (45 ns FWHM) occurring when the tube is driven at the design frequency of 11.424 GHz.

Data from the surface acoustic wave device agree with the spectrum analyzer data. Using the SAW device, small amplitude peaks in the 13–14 GHz range were seen and identified as HEM_{11} modes, also known as beam breakup or transverse displacement modes. The extremely low levels of these signals indicate that these modes are well suppressed in our tube, an important requirement for any system using a TW output structure.

Electron beam transport through the klystron was measured by beam dump calorimetry. As seen in Figure 9, the electron beam collector temperature rise is linear with repetition rate as expected. The electron beam current can be obtained from this data using the equation:

$$I_{peak} = \frac{264\Delta T Q}{r\tau V_{max}}$$

where ΔT is in $^{\circ}C$, r is the repetition rate in sec^{-1} , Q is the water flow rate in gpm and the effective pulse length, assuming space charge limited flow, is:

$$\tau = V_{peak}^{-5/2} \int_0^T V_{beam}^{5/2}(t) dt$$

where V_{beam} is the electron beam voltage, measured by a capacitive probe.

For typical operation at $V=450$ keV, the voltage pulse is similar to the one shown in Figure 4, with an effective time of $\tau = 44$ ns. Combining the data shown in Figure 9 with the measured gun perveance from Figure 4, we find electron transport through the klystron tube between 80 and 90 percent.

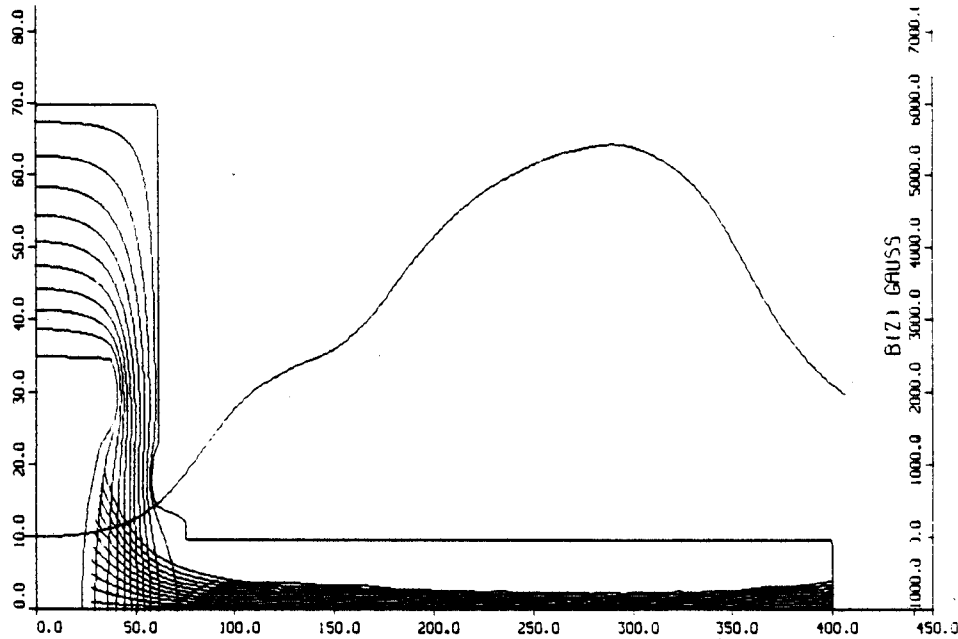


FIG. 3. Electron beam trajectories calculated by the EGUN code for the klystron and CARM experiments are shown. The axial magnetic field profile shown was obtained by maximizing the microwave power output.

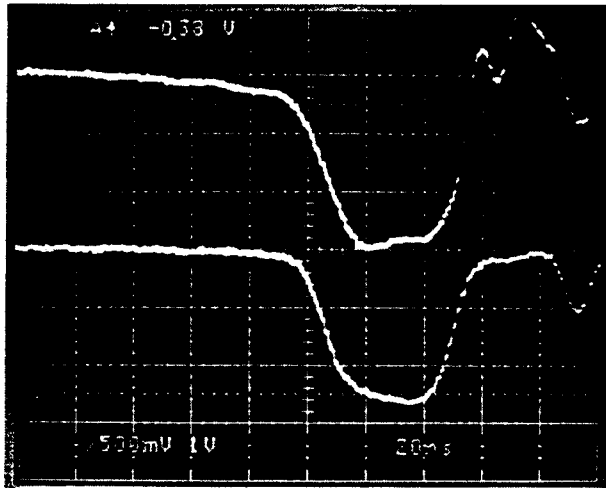


FIG. 4. Typical voltage and current waveforms for the SNOMAD-II induction accelerator are shown. Scales are 200 kV/div (top trace) and 200 A/div (bottom trace). Timescale is 20 ns/div.

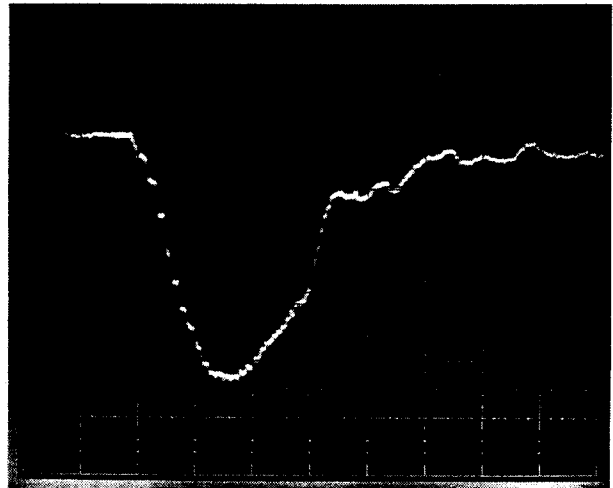


FIG. 5. Microwave signal measured by an RF diode is shown. The scale is 20 mV/div, with 87.5 mV corresponding to an output power of 100 MW. Timescale is 20 ns/div.

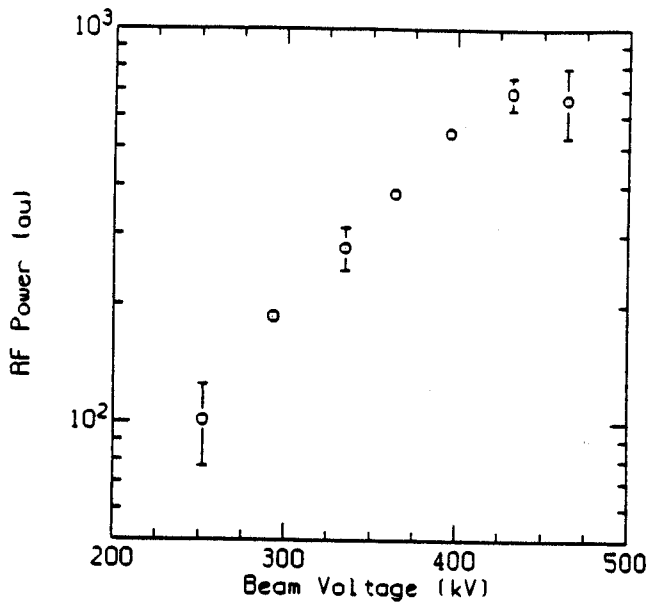


FIG. 6. The scaling of microwave power with accelerator voltage. A best fit scaling is $P \sim V^{3.6}$.

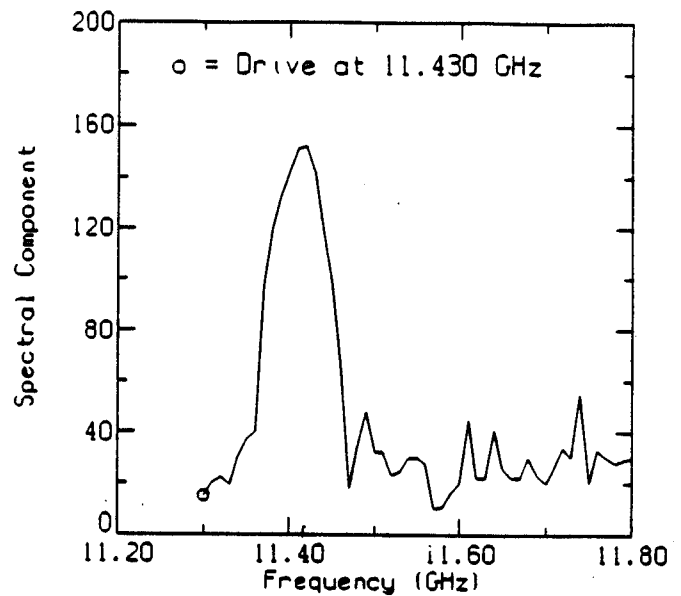


FIG. 7. When driven at 11.430 GHz only a single peak appears in the klystron output.

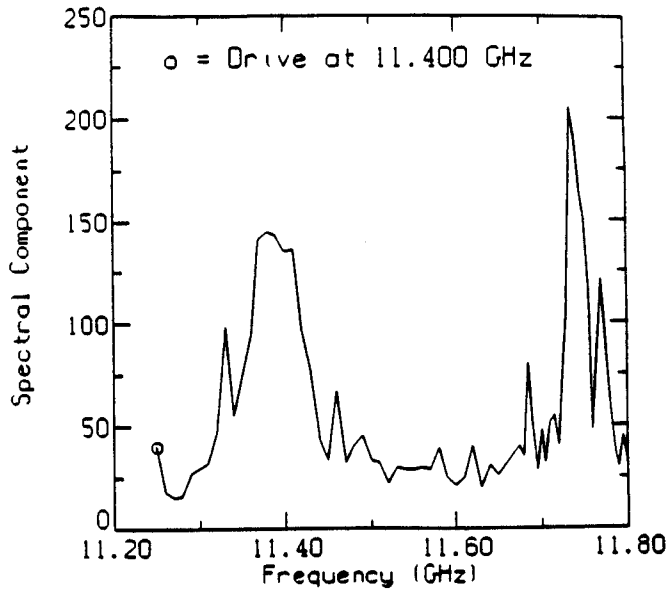


FIG. 8. When the klystron is driven at 11.400 GHz (below the nominal drive frequency) a group of frequencies near the traveling wave output π mode appear in addition to the main peak.

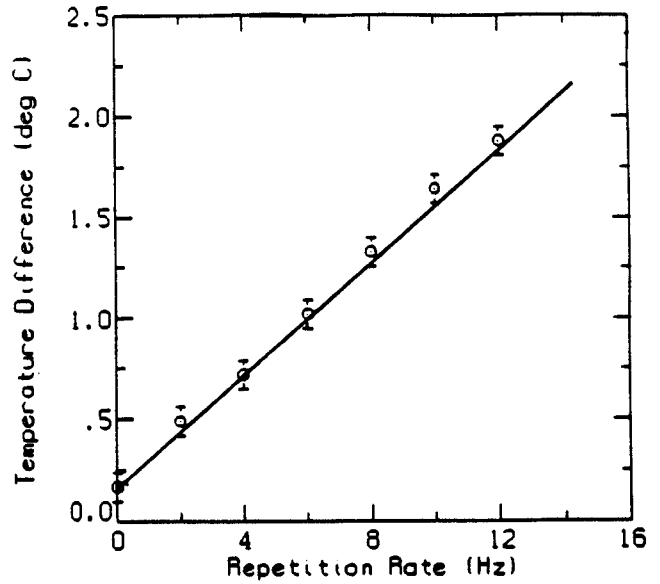


FIG. 9. The temperature rise at the klystron electron beam collector is shown as a function of repetition rate. Beam dump calorimetry is used to measure beam transport through the microwave tube.

CYCLOTRON AUTORESONANCE MASER EXPERIMENTS

The cyclotron autoresonance maser (CARM) is a novel high power RF source which utilizes the resonant interaction between a relativistic electron beam propagating in a uniform magnetic field and a wave propagating with a phase velocity slightly faster than the speed of light. Although similar to the gyrotron, the CARM interaction can extract energy from the parallel as well as perpendicular beam velocity components. CARMs are presently under investigation by several research groups in the U.S. and the Soviet Union⁸ as potentially attractive RF sources for powering the next-generation linear collider⁹ or for electron cyclotron heating of fusion plasmas.¹⁰

Design studies for a 17 GHz CARM amplifier using the 500 kV, 500 Amp SNOMAD-II Linac electron beam predict a power level of $P_{RF} \sim 25$ MW at an efficiency of $\eta \sim 10\%$. Design and simulation results for a TE_{11} mode CARM amplifier are shown in Table II. The electron beam is focused into a 2 kG axial magnetic field region where a magnetic wiggler converts parallel beam momentum to perpendicular momentum. The beam is then adiabatically compressed into the CARM interaction region to an $\alpha \equiv p_{\perp}/p_{\parallel} \sim 0.4$, where RF power amplification takes place.

Several new simulation codes were used to model both the beam transport through the microwave tube as well as model the wave-particle interaction. The beam transport from the linac to the wiggler is initially simulated with the EGUN electron trajectory program.⁵ The output from the EGUN code is then used by a new MIT beam transport code TRAJK to model the transport in the helical wiggler and CARM interaction regions.

The TRAJK code is a time-independent code which integrates particle orbits by the modified Euler's method through external magnetic fields including the effects of the transverse self-magnetic and self-electric fields from the beam. The model for the wiggler is a three-dimensional Biot-Savart integration over a user-defined current path, allowing very accurate modeling of the actual winding geometry of the bifilar helical wiggler used for imparting the perpendicular momentum to the electron beam. The axial magnetic field model includes the adiabatic compression region. At each axial position, Poisson's equations for the electrostatic potential ϕ and the vector potential A_z are solved on a polar (r, θ) grid without assuming azimuthal symmetry. Particle loading options for the code include loading from EGUN rays data, rigid-rotor and immersed-flow beam equilibria, and a relativistic Brillouin flow equilibrium. Simulation of beam formation and propagation to the CARM interaction region with the EGUN and TRAJK codes permits an accurate estimate of realistic beam velocity spread in the CARM.

Perpendicular momentum and energy spread are two key parameters which must be maintained below critical values in order to efficiently utilize the CARM interaction. The EGUN and TRAJK codes allow calculation of these parameters. Minimization of beam scalloping and optimization of the magnetic geometry are important for minimizing the beam velocity spread.

The CARM interaction is modeled with the 2-D CARM code SPOT developed at MIT. Simulations using this code show good agreement with experimental results from a 35 GHz CARM amplifier.¹¹ Figure 10 shows simulation results for the electron beam parameters listed in Table II. In this figure, the saturated efficiency is plotted versus the normalized field detuning from resonance, Δ , where

$$\Delta \equiv \frac{2}{\beta_{\perp 0}^2} \frac{1 - \beta_{\parallel 0}/\beta_{ph}}{1 - \beta_{ph}^{-2}} \left(1 - \frac{\beta_{\parallel 0}}{\beta_{ph}} - \frac{\Omega_c}{\omega}\right)$$

Beam Energy	500 keV
Beam Current	500 Amps
Pulse Length	30 ns
Velocity Ratio $\alpha \equiv p_{\perp}/p_{\parallel}$	0.4
Frequency	17.136 GHz
Mode	TE ₁₁
Guide Radius	1.3 cm
Phase Velocity β_{ph}	1.088
Axial Field Strength B_0	3.06 kG
Input Power P_{in}	800 W
Momentum Spread σ_{pz}/p_z , est.	< 1.6%
Energy Spread σ_{γ}/γ	< 1.6%
Efficiency η , untapered	13.5% ($\sigma_{pz} = 0$) 9.3% ($\sigma_{pz} = 0.02$)
Saturated Power P_{sat}	33.6 MW ($\sigma_{pz} = 0$) 23.3 MW ($\sigma_{pz} = 0.02$)
Saturated Gain Length z_{sat}	0.93 m ($\sigma_{pz} = 0$) 1.01 m ($\sigma_{pz} = 0.02$)
Amplifier Gain	46.2 dB ($\sigma_{pz} = 0$) 44.6 dB ($\sigma_{pz} = 0.02$)

Table II: Summary of the CARM operating parameters and CARM simulation results.

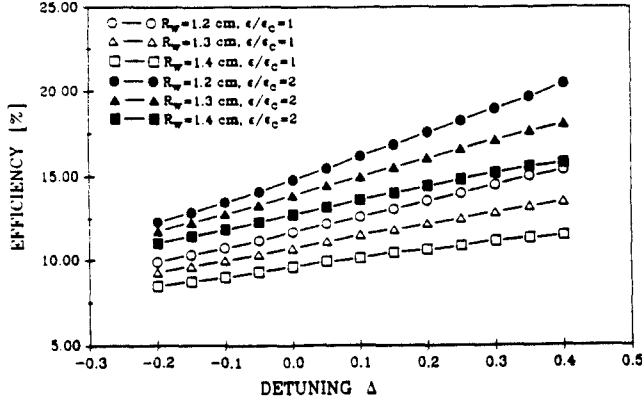


FIG. 10. Simulation of efficiency versus field detuning for a 500 kV, 500 Amp CARM parameterized by waveguide size and ratio of beam-wave coupling to critical beam-wave coupling. The beam α used is varied with detuning to maintain a given value of ϵ/ϵ_c . Simulation results are for a cold beam.

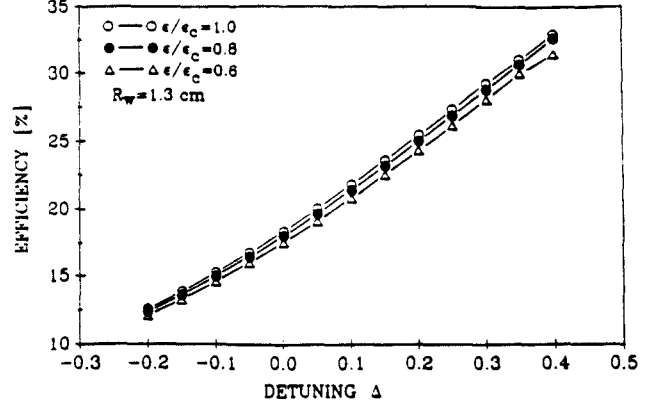


FIG. 11. Simulation of efficiency versus field detuning for a 1 MeV, 500 Amp CARM parameterized by waveguide size and ratio of beam-wave coupling to critical beam-wave coupling. The beam α used is varied with detuning to maintain a given value of ϵ/ϵ_c . Simulation results are for a cold beam.

The optimum beam α consistent with stability (see below) was chosen to be $\alpha = 0.4$; the wave phase velocity of $\beta_{ph} \equiv \omega/ck_{||} = 1.088$, corresponding to a TE_{11} mode in a 1.3 cm diameter waveguide was chosen. Other inputs to the SPOT code include the drive power $P_{in} = 800$ W and spread in beam momentum $p_z \equiv \gamma\beta_{||}$. The value of $\sigma_{pz} = 1.6\%$ used was obtained from simulations with the EGUN and TRAJK codes. The SPOT code predicts an RF source efficiency of 13.5% for a cold beam and 9.3% for the warm beam. Significant improvement in the efficiency results if the beam pitch is increased.

Long pulse Gyro-TWT amplifiers are known experimentally to be susceptible to an absolute instability, and the possibility of such an instability for a CARM amplifier must also be considered. The growth rate of the absolute instability depends on the coupling parameter¹² $\epsilon \propto (\beta_{\perp}^2/\gamma\beta_{||})(I/I_A)$, where I_A is the Alfvén current. The critical coupling ϵ_c is defined as that coupling which leads to an absolute instability on the electron beam near cutoff, according to a pinch-point analysis.¹² The design presented here is stable to an absolute instability for a beam current of 500 A and an $\alpha = 0.4$. The extent to which the beam pitch α may be increased to improve the efficiency without an absolute instability developing will depend on the relative size of the instability growth rate and the beam pulse length. For this short pulse experiment, the absolute instability may not have sufficient time to develop for α values higher than $\alpha = 0.4$. Reflections from output windows and the load will be minimized by proper design of waveguide taper regions.

The SNOMAD-II accelerator can also be configured to provide a 1 MeV, 500 Amp beam, and designs have also been carried out for a 17 GHz CARM amplifier with these beam parameters. As can be seen from Fig. 11, the predicted efficiencies are as high as 32% for a cold beam. The primary reason for the improvement in predicted efficiency between the 500 kV and 1 MeV designs is the higher attainable value of beam α for the higher voltage. Should operation with $\epsilon/\epsilon_c > 1$ prove possible with short pulses, the beam α may be increased for the 500 kV design with a corresponding increase in efficiency.

ACKNOWLEDGEMENTS

This work was supported by DARPA and monitored by NSWC under contract N60921-88-C-0234 and by the U.S. Department of Energy, Office of Basic Energy Sciences, under contract DE-FG02-89ER14052.

REFERENCES

- ¹P.B. Wilson, "High Pulse Power RF Sources for Linear Colliders," *Stanford Linear Accelerator Center Report* SLAC-PUB-3227, 1983.
- ²M.A. Allen, O. Azuma, R.S. Callin, et. al., "Relativistic Klystrons," *Stanford Linear Accelerator Center Report* SLAC-PUB-4861, 1989.
- ³*Proc. Int. Workshop on the Next Generation Collider*, Stanford Linear Accelerator Center (Nov. 1988); *Advanced Accelerator Concepts, in Conf. Proc. No. 193*, C.Joshi, Ed. New York: Amer. Inst. Phys., 1989.
- ⁴H. E. Brandt, Ed., *Proc. Society Photo-Optical Instrum. Engineers*, vol. SPIE-1061, *Microwave and Particle Beam Sources and Directed Energy Concepts*, 1989.
- ⁵W. B. Herrmannsfeldt, "EGUN - An Electron Optics and Gun Design Program", *Stanford Linear Accelerator Center Report* SLAC-226, 1979.
- ⁶J.W. Wang and G.A. Loew, "RF Breakdown Studies in Copper Electron Linac Structure," *Stanford Linear Accelerator Center Report*, SLAC-PUB-4866, 1989.
- ⁷J. Haimson and B. Mecklenburg, "Use of TW Output Structures for High Peak Power RF Generators", *Proc. Linac Conf., Albuquerque*, 1990.
- ⁸V.L. Bratman, N.S. Ginzburg, G.S. Nusinovich, M.I. Petelin and P.S. Strelkov, "Relativistic Gyrotrons and Cyclotron Autoresonance Masers," *Int. J. Electron* 51, 541-567, 1981.
- ⁹B.G. Danly, J.S. Wurtele, K.D. Pendergast and R.J. Temkin, "CARM Driver for High Frequency RF Accelerators," in F. Bennett and J. Kopta, eds. *Proc. 1989 Part. Accel. Conf.*, 223-225, I.E.E.E., 1989.
- ¹⁰M. Caplan and B. Kulke, "Design of an Induction Linac Driven CARM Oscillator at 250 GHz," in M. von Ortenberg, ed. *Conf. Digest, 14th Int. Conf. Infrared and Millimeter Waves*, 420-421, S.P.I.E., 1989.
- ¹¹G. Bekefi, A. DiRienzo, C. Leibovitch and B.G. Danly, "A 35 GHz Cyclotron Autoresonance Maser (CARM) Amplifier," *Appl. Phys. Lett.* 54, 1302-1304, 1989.
- ¹²J.A. Davies, "Conditions for Absolute Instability in Cyclotron Autoresonance Maser," *Phys. Fluids B* 1, 663-669, 1989.